MAPPING OVERBURDEN AND CAVE NETWORKS WITH MUONS. T. H. Prettyman[1], T. N. Titus[2], P. J. Boston[3], S. L. Koontz,[4] R. S. Miller,[5] [1]Planetary Science Institute (prettyman@psi.edu), [2]United States Geological Survey, Astrogeology Science Center, [3]New Mexico Institute of Mining and Technology, [4]NASA Johnson Space Center, [5]University of Alabama, Huntsville

Introduction: Muons are highly penetrating elementary particles (leptons) that are produced by galactic-cosmic-ray showers in Earth's upper atmosphere. Relativistic muons are abundant at sea level and can penetrate, virtually undeflected, through hundreds of meters of rock. Over a hundred muons per second pass through every square meter of Earth's surface [e.g. 1], providing an intense and relatively-uniform source of ionizing particles, which can be used to probe the internal structure of large objects (e.g., pyramids, volcanos, and nuclear reactor cores) [2-4]. A simple gauge can be used to measure overburden thickness. Muons were used for this purpose in the 1950s for civil engineering [5] and recently to map the density of geologic units using existing roadway tunnels [6].

Here, we summarize research on muon gauges and imaging systems used to characterize caves and cave networks on Earth and, prospectively, on Mars, the Moon, asteroids, and other planets (Fig. 1). Specific uses for muography include measurements of overburden and imaging unknown but suspected cavities. Overburden can influence the cave energy balance [7]. Shielding provided by caves has implications for astrobiology [8]. Caves could provide a natural shelter from space radiation for long term human settlements envisioned for the Moon and Mars [9]. If compact, inexpensive instruments can be deployed, muons could be a powerful tool for speleologists.

Overburden gauge: Overburden can be determined by measuring downward-going atmospheric muons arriving at a detector deployed inside a cave (**Fig. 1**). The flux of atmospheric muons at Earth's surface is well-known [e.g. 1] (**Fig. 2**). The range of muons increases with kinetic energy. High-energy muons are capable of penetrating many km of rock [3]; however, above about 1 GeV, the flux of muons decreases with kinetic energy. Consequently, long-range muons comprise a small part of the roughly 0.01 muons/cm^2/s/sr arriving at Earth's surface from the zenith.

The overburden gage illustrated in **Fig. 1**, counts muons arriving within a well-defined acceptance angle about zenith. The muon counting rate is given by the product of the vertical muon flux above a threshold kinetic energy and the étendue of the counter, given by the product of the area of the detector (A) and solid angle of acceptance (Ω), with units of cm^2-sr.

All muons within the energy range shown in **Fig. 2** will trigger the counter. As the overburden increases, a

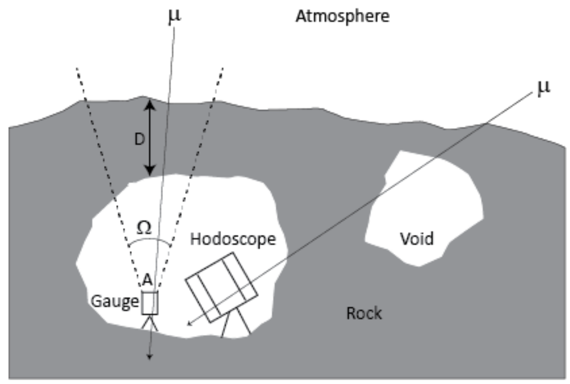

Figure 1. Cave-deployed gauge to determine overburden (D in g/cm^2) and hodoscope to search for voids nearby. The response of the gauge depends on the acceptance area A (cm^2) and solid angle Ω (steradians, abbreviated sr). Example trajectories of atmospheric muons (μ) through the surrounding medium are shown. The hodoscope ("hodos" + "skopos" = path + observer) makes use of imaging planes to determine the direction of incident muons. A radiograph of the rock formation intervening between the cave and sky can be accumulated from multiple muon hits.

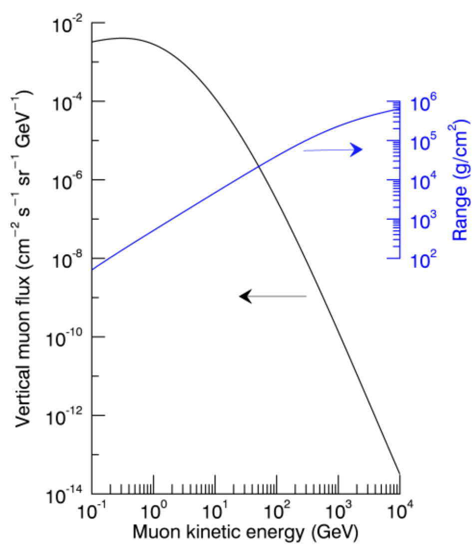

Figure 2. The energy distribution of muons at sea level [1] is compared with their range in g/cm^2. Dividing by density gives range in cm. Within the energy range shown, the highest-energy muons can penetrate several km through rock; whereas the lowest energy muons are stopped in a few decimeters. The total flux of vertical muons Φ_v at sea level is about 0.01 cm^{-2} sr^{-1} s^{-1}.

portion of the low energy muons range out, reducing the vertical flux at depth. The transmission T is the ratio of the vertical flux at the surface to the flux at depth (**Fig. 3**). Transmission can be determined from the counting rate C measured at depth ($C=\Phi_v A\Omega T$). The counting rate decreases monotonically with increasing overburden.

A portable gauge with an area of 100 cm^2 and 20° half-angle cone opening (étendue of about 40 cm^2-sr) gives a surface counting rate of about 1400 hr^{-1} (3% relative uncertainty in counts in 1 hr). At a depth of 2000 g/cm^2 (10 m for rock density of 2 g/cm^3), about an hour of accumulation time is required to achieve a precision of 100 g/cm^2 (half a meter). Several hours of accumulation are required to achieve the same precision at 20 m depth. Practical measurements of overburden, up to a few 10s of meters, are possible using this gauge.

Finding hidden caves: A hodoscope, which measures muon trajectories, is required to radiograph the surrounding rock formation or structures near the cave (**Fig. 1**) [2]. A 1000 cm^2 hodoscope was developed and demonstrated by [10] for this purpose. The field of view depends on local terrain. Measurements at multiple locations within one or more caves could enable tomographic imaging of portions of a cave network.

Hodoscopes consist of two or more tracking planes from which the direction of each muon is reconstructed. The accumulation of many muon tracks enables the formation of a radiograph of transmitted muons, which can be converted into an image of chord-lengths (g/cm^2, **Fig. 3**) transected by the muons as they pass through the rock. Long counting times are required for imaging; however, with patience, high-contrast sensitivity and resolution can be achieved using Earth's atmospheric muons [e.g. 2-4, 10].

Extraterrestrial caves: Fewer vertical muons are made in the thin atmosphere of Mars; however, the horizontal flux of muons at the surface is expected to be higher than for Earth, which is advantageous for imaging [11]. The thin atmosphere poses other challenges. Primary galactic cosmic rays and secondary particles other than muons are abundant at the surface. For measurements on the surface, special considerations are needed in order to separate transmitted muons from this background, which may increase the complexity of the hodoscope [11]. The shielding afforded by a cave (at depths greater than 1000 g/cm^2, equivalent to sea level on Earth) would reduce this background, perhaps enabling the use of relatively simple hodoscopes demonstrated for Earth applications.

Similarly, on the Moon, caves might provide a low-background environment for muon measurements; however, the Moon lacks an atmosphere. Muon production in solid materials is orders of magnitude lower than in Earth's atmosphere. In addition, muon production depends on regolith density, within the top meter of the surface [12]. Special instrumentation, long integration times and corrections for topography and surface density (e.g., using radar) would be needed in order to image the formation around a lunar cave or nearby geologic features. Such measurements, nonetheless, could provide useful information for geology and civil engineering (e.g. verification of structural integrity) by future lunar explorers and inhabitants. The application of muon imaging to characterize the interior of small airless bodies (e.g., asteroids and comets) is the subject of a Phase II NASA Innovative Advanced Concepts (NIAC) project [12].

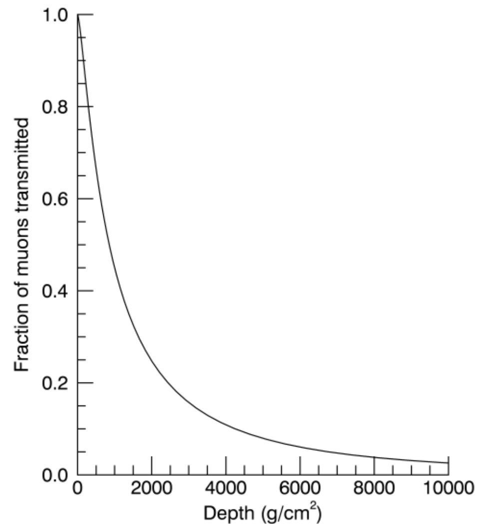

Figure 3. The fraction of muons T transmitted through standard rock. The transmission depends on the initial energy distribution of muons (the vertical flux at sea level, shown in Fig. 2).

References: [1] Allkofer, O. et al. (1971), *Phys. Lett.*, 36B(4), 425-427. [2] Alvarez, L. W. (1970), Science, 167, 832-839. [3] Tanaka, H. K. M. (2010), *Earth Planets Space*, 62, 119-129. [4] Miyadera H. (2013) *AIP Advances*, 3, 052133, doi: 10.1063/1.4808210. [5] George, E. P. (1955), *Commonwealth Engineer*, 455. [6] Tanaka, H. K. M. (2015), *Sci. Rep.* 5: 8305, doi: 10.1038/srep08305. [7] Titus T. N. et al. (2010) *LPS XXXXI*, Abstract #1096. [8] Levelle R. J. and Datta S. (2010) *PSS*, 58, 592–598. [9] Boston, P. J. et al. (2003), *Gravit. Space Biol. Bull.*, 16(2), 121-131. [10] Olah, L. et al. (2012), *Geosci. Instrum. Method. Data Syst.*, 1, 229–234. [11] Kedar et al. (2013), *Geosci. Instrum. Method. Data Syst.*, 2, 157–164. [12] Prettyman et al. (2014), NASA/NIAC Phase I Final Report.